Effect of vitronectin-derived functional peptides on the bone healing capacity of microroughened titanium surfaces

2020년

조 창 빈

치의과학박사 학위논문

Effect of vitronectin-derived functional peptides on the bone healing capacity of microroughened titanium surfaces

인체유래 부착단백질 비트로넥틴에서 발굴한 기능성 펩타이드가 미세거칠기를 증가시킨 티타늄 임플란트 표면의 골형성능에 미치는 영향

2020년 8월

서울대학교 대학원

치의과학과 치과보철학 전공

조 창 빈

치의과학박사 학위논문

Effect of vitronectin-derived functional peptides on the bone healing capacity of microroughened titanium surfaces

인체유래 부착단백질 비트로넥틴에서 발굴한 기능성 펩타이드가 미세거칠기를 증가시킨 티타늄 임플란트 표면의 골형성능에 미치는 영향

2020년 8월

서울대학교 대학원

치의과학과 치과보철학 전공

조 창 빈

Effect of vitronectin-derived functional peptides on the bone healing capacity of microroughened titanium surfaces

지도교수 여 인 성

이 논문을 치의과학박사 학위논문으로 제출함

2020년 5월

서울대학교 대학원
치의과학과 치과보철학 전공
조 창 빈

조창빈의 박사학위논문을 인준함

2020년 7월

위원장 (인)

부위원장 (인)

위 원 (인)

위 원 (인)

위 원 (인)

Abstract

Effect of vitronectin-derived functional peptides on the bone healing capacity of microroughened titanium surfaces

Chang-Bin Cho, DDS, MSD
Program in Prosthodontics, Department of Dental Science,
The Graduate School, Seoul National University
*(Directed by Prof. **In-Sung Yeo**, DDS, MSD, PhD)*

Objectives. Although sandblasted, large-grit, acid-etched (SLA) titanium surface implants have demonstrated excellent osseointegration in clinical dentistry, there still exists a need to improve SLA titanium surface modification for achieving earlier implant loading and stronger osseointegration under unfavorable systemic status. In this study, we investigated the effect of a vitronectin-derived functional peptide, VnP-16, on early bone healing capacity by applying the peptide to an SLA titanium surface implant in vivo. An in vitro experiment was also done with osteoblast-like cells.
Methods. The following four surface types of titanium disks were prepared to evaluate surface topography and chemistry: polished (control), SLA, scrambled peptide-treated, and VnP-16-treated. Cellular responses, including attachment, spreading, migration, and viability of human osteosarcoma (HOS) and MG-63 cells, were evaluated in vitro on multiwell culture plates. Next, the following four types of titanium implant surfaces were prepared for in vivo experiments: turned (control), SLA, scrambled peptide-treated, and VnP-16-treated. The implants were inserted into the tibiae of four New Zealand white rabbits according to the split plot design. After 2 weeks of implant placement, the experimental animals were sacrificed and the tibiae were removed en bloc with the implants. The undecalcified specimens were prepared and the histomorphometric data were measured using a light microscope. Analysis of variance tests were used to compare the mean values at a significance level of 0.05.
Results. VnP-16 treatment had no significant effect on the micro-topographical features of the titanium disk surfaces. VnP-16 treatment accelerated the attachment and spreading of human osteoblast-like cells and hardly affected the proliferation of cell viability and cytotoxicity. The VnP-16-treated SLA implants exhibited no foreign body reaction at the bone-implant interfaces and revealed remarkable bone-to-implant contact ratios, whose mean value was significantly higher than that in the SP-treated implants ($p = 0.027$).
Conclusions. VnP-16 enhances the osteogenic potential of microroughened SLA titanium dental implant surfaces.

Keywords: vitronectin; peptides; cell adhesion; titanium; osseointegration; dental implants; biocompatible materials
Student Number: 2014-30702

CONTENTS

Effect of vitronectin-derived functional peptides on the bone healing capacity of microroughened titanium surfaces

Chang-Bin Cho, DDS, MSD

Program in Prosthodontics, Department of Dental Science,
The Graduate School, Seoul National University
*(Directed by Prof. **In-Sung Yeo**, DDS, MSD, PhD)*

1. Introduction

Normal implant function in patients' bodies is possible only when successful osseointegration is achieved at the bone-implant interface. Biocompatible titanium is the material of choice in dental implants at present, and microroughened surfaces of commercially pure titanium have been globally used in dental clinics.[1] Sandblasted, large-grit, acid-etched (SLA) surface with approximately 1.5 μm of arithmetical mean deviation induces faster bone healing at the bone-implant interface than the turned surface with no modification.[2-4] Although SLA surface implants have demonstrated more outstanding results in terms of osseointegration than the turned surface, the average time required to load masticatory force on the inserted implants is considered to be approximately 6 weeks at least.[5,6] Moreover, depending on the patient's systemic condition, it is essential to wait for more time for osseointegration, and even if a longer time of more than 12 weeks has elapsed, the early failure of an implant, or osseointegration failure, does occur. Hence, there is still a strong need to improve SLA titanium surface modification for achieving earlier implant loading and stronger osseointegration under an unfavorable systemic status.

When a dental implant is installed into the drilled site of a jaw bone, the titanium implant surface gets soaked with blood and calcium ions adhere to the hydrated implant surface. As the surface polarity of the titanium changes to positive charge under the influence of calcium ions, several plasma proteins, primarily albumin, combine with the surface via the calcium ions. Gradually, extracellular matrix (ECM) proteins, including vitronectin, which play a major role in cell attachment, are substituted for albumin.[7] As osteogenic cells have a strong affinity to these ECM proteins, the application of these ECM

proteins on a titanium surface leads to faster and stronger osseointegration.

Vitronectin contributes to the healing of the peri-implant bone by promoting the attachment and spreading of the osteogenic cells, which implies that vitronectin reorganizes the intracellular microfilaments and microtubules, thereby facilitating cell attachment and spreading.[7-11] However, the use of such an original protein is limited: the cost for synthesis is expensive, such a macromolecule is antigenic and unstable, and moreover, this macromolecule spatially interferes with focal adhesion.[12-14] A functional peptide derived from the parent protein is a notable alternative that can overcome these limitations and maintain the original biological activity.[8,12,13,15-17] Furthermore, bioactive peptides are more favorable than larger protein molecules due to their robustness and sterilizability.[18] Recently, a vitronectin-derived functional peptide sequence, RVYFFKGKQYWE [residues 270-281 (Arg-Val-Tyr-Phe-Phe-Lys-Gly-Lys-Gln-Tyr-Trp-Glu, VnP-16)], has demonstrated numerous beneficial effects on bone formation.[8] The peptide VnP-16 promotes osteogenic cell behaviour, including cell attachment and spreading, to an extent that is comparable to that promoted by vitronectin. A specific adhesion receptor, β1 integrin, on the human osteogenic cell surface is a major surface transmembrane receptor for VnP-16 and effectively mediates the VnP-16-induced osteogenic cell attachment and migration. VnP-16 also promotes bone formation by enhancing osteoblast differentiation through focal adhesion kinase phosphorylation and by proliferating osteoblasts. Concomitantly, the peptide inhibits bone resorption by restraining the osteoclast differentiation of Janus N-terminal kinase-c-Fos-nuclear factor of activated T cells, (NFATc1) and the resorptive function of αvβ3 integrin-c-Src-proline-rich tyrosine kinase 2 (PYK2). Moreover, VnP-16 decreases the bone resorption activity of preexisting mature osteoclasts without changing their survival rate.[8]

Functionalization of a titanium implant through the immobilization of desirable proteins or bioactive peptides is a promising approach to overcome the bioinertness of the titanium surface, leading to enhanced osseointegration.[18,19] Nevertheless, controversy exists regarding the methods used for immobilizing bioactive peptides on experimental surfaces. Several methodologies, including physical adsorption and covalent immobilization, have been investigated since the beginning of protein functionalization on titanium substrates.[19] Among these, physical adsorption is the simplest method for immobilizing proteins on titanium substrates. It can be achieved by physical contact with a protein-containing medium, either intentionally through a simple drop of the protein solution on the substrate or through immersion of the substrate into the protein solution for a given time. The primary advantage of physical adsorption is that it can be easily implemented by virtue of the simplicity of the process. However, physical adsorption presents several disadvantages, including that the effective concentration of the protein, the quantity interacting with the substrate per unit area, is low.[19] Chemical covalent immobilization is the most established of the protein functionalization approaches, which enables permanent attachment of proteins to titanium substrates, overcoming the unintentional protein release, which is a problem in adsorption approaches. It can be achieved through a separate linker molecule that mediates the chemical covalent bond between the protein and the substrate. The primary issue associated with chemical covalent immobilization is the process complexity requiring at least three steps and long reaction time. The technique also lacks scalability and

reproducibility, which implies that the reaction situation is uncommon in the manufacturing environment.[19] Physical covalent immobilization of biomolecules is the most recent approach to dental and orthopedic biomimetic functionalization, referred to as plasma-based technology that infiltrates ionic species into the substrate or coats the substrate with the additional layer of a new material. This physical approach is superior to adsorption and chemical covalent immobilization because of its versatility and substrate independence. However, providing infrastructures, including power supplies and vacuum systems, incurs a tremendous expense, and the plasma treatment has not yet been successfully applied for coating complex 3D structures with cavities and shadowed irregularities such as internal porosity.[19]

Functionalization of VnP-16 to microroughened SLA titanium surface increases clinical relevance in further enhancement of bone healing and makes the indication of dental implant treatment extended to patients suffering from a bone metabolic weakness such as osteoporosis. However, the VnP-16-treated SLA titanium surface has not yet been investigated. Therefore, this study was conducted to examine the effect of VnP-16 on early bone healing capacity by applying it to microroughened SLA titanium surface implant in vivo. In vitro experiments were also conducted using osteoblast-like cells. The hypothesis underlying this study was that treatment with VnP-16 would further accelerate the osteogenic potential of the microroughened SLA titanium surface.

2. Materials and Methods

2.1. Cells, Peptides, and Reagents

Osteoblast-like HOS and MG-63 cells, lines derived from human osteosarcomas, were purchased from the American Type Culture Collection (Rockville, MD, USA) and cultured in Dulbecco's modified Eagle's medium (Gibco BRL, Carlsbad, CA, USA) supplemented with 10% fetal bovine serum (Table 1). The VnP-16 peptide (RVYFFKGKQYWE) and a scrambled peptide (SP) were synthesized using the 9-fluorenylmethoxycarbonyl-based solid-phase method with a C-terminal amide using a Pioneer Peptide Synthesizer (Applied Biosystems, Foster City, CA, USA). The scrambled peptide as a negative control had a randomly determined sequence through a pilot test, which demonstrated a minimal effect on cell attachment. The peptides were characterized and purified by Peptron (Daejeon, Korea). The peptides used in this study had a purity >95%, as determined using high-performance liquid chromatography (Table 2). Human plasma vitronectin was obtained from Millipore (Bedford, MA, USA) (Table 3).

Table 1. General information of the cells used in this study.

Cell	Organism	Tissue	Product Format	Morphology	Culture Properties
HOS	Human	Bone (osteosarcoma)	Frozen	Mixed, fibroblast, and epithelial-like cells	Adherent
MG-63	Human	Bone (osteosarcoma)	Frozen	Fibroblast	Adherent

Table 2. Peptides used in this study.

Peptide	Molecular Formula	Amino Acid Sequence	Purity
VnP-16	$C_{82}H_{112}N_{20}O_{17}$	R-V-Y-F-F-K-G-K-Q-Y-W-E-NH_2	95%
VnP-16-SP10*	$C_{82}H_{112}N_{20}O_{17}$	F-V-W-R-Q-F-Y-K-Y-E-K-G-NH_2	98%

* VnP-16-Scrambled Peptide 10

Table 3. Biological information of vitronectin.

Protein	Source	Size	Application recommended
Vitronectin	Human plasma	478 amino acids	1 μg/mL in cell attachment assays

2.2. Disk Preparation and Surface Characterization

Titanium disk specimens, which were 0.5 mm in thickness and 20 mm in diameter, were made of commercially pure grade 4 titanium. The control disks were prepared by polishing with #600 and #1200 sandpaper. The other disk surfaces were sandblasted with large alumina (Al_2O_3) grit and etched with hydrochloric acid solution (Deep Implant System, Seongnam, Korea). These sandblasted, large-grit, acid-etched (SLA) titanium disks were rinsed, ultrasonically washed, and dried. One group of the SLA disks was left untreated, another was treated with a scrambled peptide (SP; 10.5 μg/cm^2), and the other was treated with VnP-16 (10.5 μg/cm^2).

The surfaces of the four types of disks were imaged by field emission scanning electron microscopy (FE-SEM; S-4700, Hitachi, Tokyo, Japan). Confocal laser scanning microscopy (CLSM; LSM 800, Carl Zeiss AG, Oberkochen, Germany) was used to calculate two surface parameters for surface topography of the disk specimens, i.e., arithmetical mean height (Sa) and developed surface area ratio (Sdr).[20] The surface chemistry in each group was analyzed by x-ray photoelectron spectroscopy (XPS; Sigma Probe, Thermo Scientific, Waltham, MA, USA).

2.3. Cell Attachment and Spreading Assays

Cell attachment assay was performed using 24-well culture plates (Figure 1A).[8] The physical adsorption method was used for the application of vitronectin and peptides. Each culture plate was coated with 0.26 μg/cm^2 human plasma vitronectin for 24 h at 4°C or with 10.5 μg/cm^2 SP or 10.5 μg/cm^2 VnP-16 for 24 h at room temperature, blocked with 1% heat-inactivated bovine serum albumin (BSA) in phosphate-buffered saline (PBS) for 1 h at 37°C, and then washed with PBS. Cells (1×10^5/500 μL) were added to each plate and incubated in serum-free culture medium for 1 h at 37°C. After the incubation period, unattached cells were removed by rinsing twice with PBS. Attached cells were fixed with 10% formalin for 15 min, stained with 0.5% crystal violet for 1 h, gently washed with distilled water three times, and dissolved using 2% sodium dodecyl sulfate for 5 min. The absorbance was measured at 570 nm using a Model 550 microplate reader (Bio

Rad, Hercules, CA, USA). For cell-spreading assay, cells (7×10^4/500 μL) were added to each substrate-coated plate and incubated for 3 h at 37°C. To determine the degree of cell spreading, cell-cultured, formalin-fixed, crystal violet-stained, and distilled water-washed culture plates were photographed using a light microscope (DS-Ri2, Nikon, Tokyo, Japan) at a magnification of ×400, and the spread cell surface area was measured using the Image-Pro Plus software (Version 4.5; Media Cybernetics, Silver Spring, MD, USA). The total area occupied by 100 cells on each measured field was estimated, and the mean and standard deviation of the areas were calculated.[20]

2.4. Cell Migration Assay

Cell migration assay was performed using a transwell migration chamber (Corning Inc., Pittston, PA, USA) with polycarbonate filter (pore size, 8 μm).[21] The lower side of each transwell filter was coated with vitronectin (0.26 μg/cm^2), SP and VnP-16 (10.5 μg/cm^2) by drying for 24 h at 4°C (vitronectin) or for 24 h at room temperature (peptides). Cells (2×10^4/24-well) were seeded in the upper chamber of a transwell filter and allowed to migrate for 24 h at 37°C (Figure 1B). Cells were then fixed with 10% formalin for 15 min and stained with 0.5% crystal violet. Unmigrated cells in the upper side of the transwell filter were removed using a cotton swab, and cell migration was quantified by counting the number of cells at the lower side of the filter that had penetrated through the filter under a light microscope (DS-Ri2, Nikon, Tokyo, Japan) at a magnification of ×400. Vitronectin served as the positive control, and SP as the negative control.

2.5. Cell Viability Assay

Cell viability was evaluated using the EZ-Cytox Cell Viability Assay kit (water-soluble tetrazolium salt method; DoGenBio Co., Ltd, Seoul, Korea). The EZ-Cytox is a useful kit that accurately measures cell viability in a far easier and simpler manner than the MTT assay using the water-soluble tetrazolium salt. A 96-well culture plate was coated with VnP-16 peptide (0, 10.5, 21.0, or 42.0 μg/cm^2) by drying for 24 h at room temperature. Cells (1.5×10^4/100 μL) were seeded onto the culture plate and then incubated for 24 or 48 h at 37°C. The water-soluble tetrazolium salt reagent solution (10 μL) was added to each well, and the plate was incubated for 2 h at 37°C. The absorbance was then measured at 450 nm using a microplate reader.

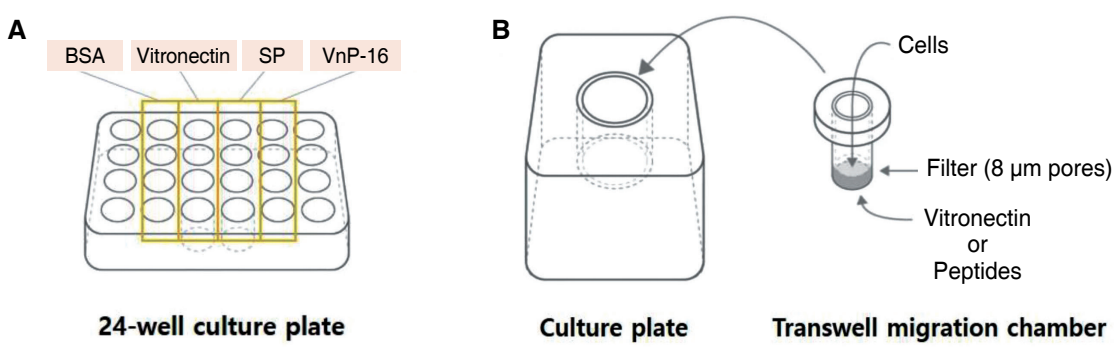

Figure 1. Schematic drawing of 24-well culture plate **(A)** and transwell migration chamber with polycarbonate filter possessing 8 μm pores **(B)**.

2.6. In Vivo Experiment

A total of 16 screw-shaped grade 4 titanium implants were prepared, which were 3.5 mm in diameter and 11 mm in length (Warantec, Seongnam, Korea). The groups classified according to the surfaces are shown in Table 4. The peptide-treated implants were placed on 0.2 ml PCR tubes and coated with SP or VnP-16 peptide (1.0 mg/cm^2) by drying for 7 days in a vacuum at room temperature.[15] All the animal experiments performed in this study were approved by the Ethics Committee of Animal Experimentation of the Institutional Animal Care and Use Committee (CRONEX-IACUC 201705001; Cronex, Hwasung, Korea). These experiments were conducted according to the Animal Research: Reporting In Vivo Experiments (ARRIVE) guidelines for the care and use of laboratory animals.[22] Four New Zealand white male rabbits aged approximately 5-6 months and weighing 2.5-3.0 kg were used in this study. The rabbits were intramuscularly anesthetized with a dose of 15 mg/kg tiletamine hydrochloride and zolazepam hydrochloride (Zoletil, Virbac, Carros, France) and 5 mg/kg xylazine (Rompun, Bayer AG, Leverkusen, Germany). The skin hair was shaved at the tibial area of the rabbits, which was disinfected with iodopovidone. A full-thickness incision was made from the skin to the periosteum of the tibiae, and the medial surfaces of the tibiae were exposed by elevation of the flaps. The holes for implant insertion were prepared by sequential drilling: 2-mm, 2.5-mm, 2.7-mm and 3.2-mm (final) diameter twist drills were used. Two implants were inserted into each tibia and four implants were received by each rabbit. According to the split plot design, one implant from each group was placed (Figure 2). The periosteum and fascia were sutured with 4-0 polyglactin 910 (Vicryl, Ethicon, Somerville, NJ, USA), and the skin was sutured with 4-0 Nylon (Ethilon, Ethicon, Somerville, NJ, USA). Each experimental animal was housed in a separate cage, and a fluoroquinolone antibiotic (Enrofloxacin; Biotril, Komipharm International, Siheung, Korea) was administered to prevent infection.

2.7. Histomorphometry

The experimental animals were sacrificed under general anesthesia with the intravenous administration of KCl at 14 days after implant surgery. The implants were removed en bloc with the surrounding bones and fixed in 10% neutral buffered formalin for 2 weeks. After formalin fixation, each implant-bone block was dehydrated with ethanol. Then, the blocks were embedded into resin (Technovit 7200, Heraeus Kulzer, Hanau, Germany) and ground for light microscopy using the EXAKT system (EXAKT

Table 4. The implants investigated in this study.

	Surface	N
Group A	No modification (turned, control)	4
Group B	Sandblasted, large-grit, acid-etched (SLA*)	4
Group C	SLA* treated with SP (1.0 mg/cm^2)	4
Group D	SLA* treated with VnP-16 (1.0 mg/cm^2)	4

* Deep Implant System, Seongnam, Korea

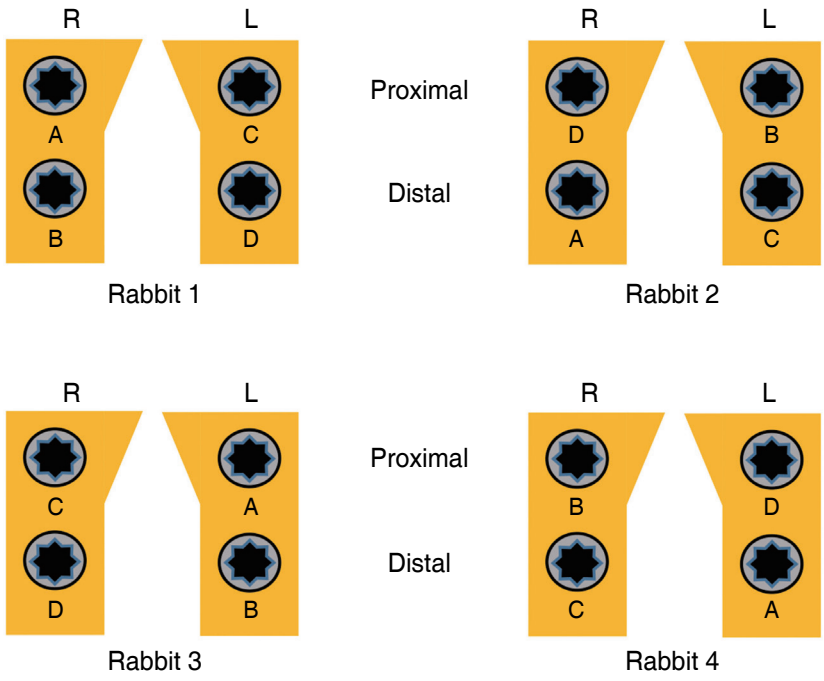

Figure 2. Different implants were placed in the rabbit tibiae according to a split-plot design under the assumption that all rabbits had identical conditions (A = turned; B = SLA; C = SP; D = VnP-16). Turned = turned surface; SLA = sandblasted, large-grit, acid-etched surface; SP = SLA surface treated with SP; VnP-16 = SLA surface treated with VnP-16.

Apparatebau, Norderstedt, Germany) according to methods described in previous studies.[20,23] Sections of the implant-bone blocks, which was approximately 50 μm in final thickness, were prepared and subjected to modified Goldner's Masson trichrome staining.[24] The interfacial areas between the bones and implants were observed and evaluated from the bone crests to 2 mm in depth for histomorphometry. Bone-to-implant contact (BIC) and bone area (BA) ratios were measured. The images were analyzed and histomorphometric data were obtained using a light microscope (BX51, Olympus, Tokyo, Japan) and the SPOT version 4.0 software (Diagnostic Instruments, Sterling Heights, MI, USA) and Image-Pro Plus (Media Cybernetics, Rockville, MD, USA).

2.8. Statistical Analyses

Descriptive statistics for the data were presented as mean ± standard deviation (SD). Statistical analyses were performed using the R software (version 3.6.1, R Foundation for Statistical Computing, Vienna, Austria). The normal distribution of all the data was confirmed by the Shapiro-Wilk test. Analysis of variance (ANOVA) tests were used to compare means among the groups. When a significant difference was found, Tukey's honestly significant difference test was further applied for pairwise comparisons. The level of significance was 0.05 in this study.

3. Results

3.1. Surface Characteristics

The FE-SEM images of the specimens exhibited extremely different topographical features between the polished and SLA surfaces (Figure 3A). Some grooves were found on the overall flat surfaces of the polished specimens, whereas many honeycomb-like irregularities were observed in the SLA specimens. The treatments with SP and VnP-16 had almost no effect on the surface topographical features of the surfaces (Figure 3A). No significant difference was detected in either Sa or Sdr among the SLA titanium disks regardless of the peptide treatment ($p > 0.05$) (Figure 3B). However, with respect to surface chemistry, it was confirmed that treatments with the functional peptides resulted in higher nitrogen contents on the SP- and VnP-16-treated surfaces than those in the other groups with no peptide treatment ($p < 0.05$) (Figure 3C).

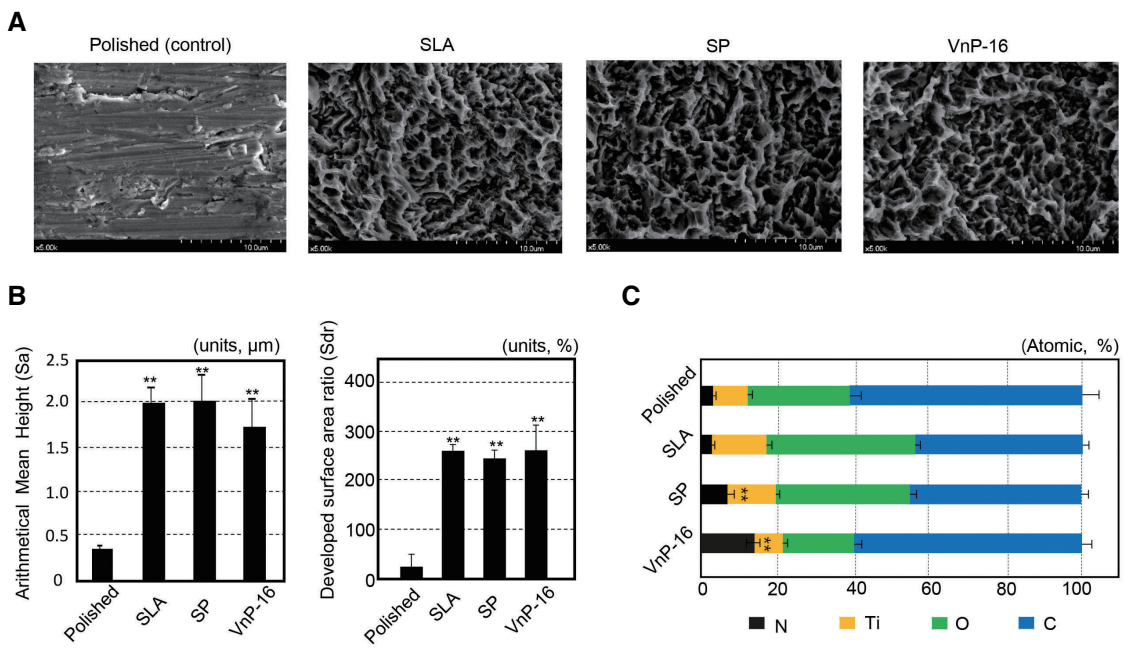

Figure 3. Surface topography and chemistry of the titanium specimens investigated in this study. **(A)** Field emission scanning electron microscopy clearly reveals different topographical features between the polished and sandblasted, large-grit, acid-etched (SLA) surfaces. **(B)** The mean values of the measured surface parameters indicated that peptide treatment did not change the surfaces physically at the micro level. Significant differences could be observed in the surface parameters between the polished and the other SLA surfaces. ** $p < 0.05$ vs. the polished surface. **(C)** X-ray photoelectron spectroscopy detected high nitrogen content on the peptide-treated surfaces. Almost no nitrogen was found in the other groups. ** $p < 0.05$ vs. the polished and SLA surfaces (significant differences are marked only for the nitrogen content).

3.2. Effects of VnP-16 Peptide on Cellular Responses of Human Osteosarcoma Cells

We investigated whether the human vitronectin-derived peptide VnP-16 could mediate cell attachment, spreading, and migration of human osteoblast-like cells. Human osteosarcoma (HOS) and MG-63 cells were used in this study. The attachment of the osteoblast-like cells was evaluated using a cell adhesion assay in serum-free medium. The responses of HOS cells to the materials are shown in Figure 4A. Human plasma vitronectin was found to strongly promote cell attachment (Figure 4A(b), B) and spreading (Figure 4A(f), C) in osteoblast-like HOS cells. The peptide VnP-16 also showed significantly enhanced cell attachment (Figure 4A(d), B) and spreading (Figure 4A(h), C), compared to BSA or SP control, and its attachment and spreading activities were comparable to those of vitronectin (Figure 4A-C). BSA and SP had little effect on the migration of HOS cells. Conversely, vitronectin and VnP-16 promoted HOS cell migration, although the former was significantly more effective than the latter (Figure 4D). The peptide VnP-16 affected the proliferation or viability of HOS cells but with no significance (Figure 4E), indicating that its stimulatory effect on the behaviour of HOS cells was due to neither cytotoxicity nor enhanced cell proliferation. These results support that VnP-16 is functionally active in increasing osteoblastic responsiveness.

3.3. Effects of VnP-16 on Cellular Responses of Human Osteoblast-like MG-63 Cells

In order to determine whether the effects of the peptide VnP-16 on the behaviour of HOS cells were similar to those on other human osteoblast-like cells, we used human osteoblast-like MG-63 cells. Similar results were found for the behaviour of MG-63 cells (Figure 5A). Human plasma vitronectin and VnP-16 had strong positive effects on cell attachment (Figure 5A(b), 5A(d), B) and spreading (Figure 5A(f), 5A(h), C) in MG-63 cells, compared with BSA or SP control. VnP-16 was comparable to vitronectin in both the cell attachment and spreading activities (Figure 5A-C). VnP-16 had no significant influence on the proliferation or viability of MG-63 cells, which was similar to the result for HOS cells (Figure 5D). However, the effects of vitronectin and VnP-16 on the migration activities of MG-63 cells were different from those of HOS. The migration of MG-63 cells was unaffected by vitronectin and VnP-16 (data not shown). Taken together, the responses of the HOS and MG-63 cells to VnP-16 treatment were different in terms of cell migration but similar in terms of cell attachment, spreading, and viability.

3.4. Histomorphometry

All the experimental animals were healthy, and neither signs of diseases nor pathological states were found until the sacrifice. Moreover, no special inflammatory or immune cells were found in the light microscopic view of the specimens. After 14 days of implant insertion, sufficient mineralization was detected in each section (Figure 6A). The mean values and SD in the histomorphometric data are shown in Table 5. The one-way ANOVA test found a significant difference in BIC ($p = 0.027$). However, the pairwise comparisons between the groups failed in detecting any significant difference (Figure 6B). There were no significant differences in BA among the groups (Figure 6C).

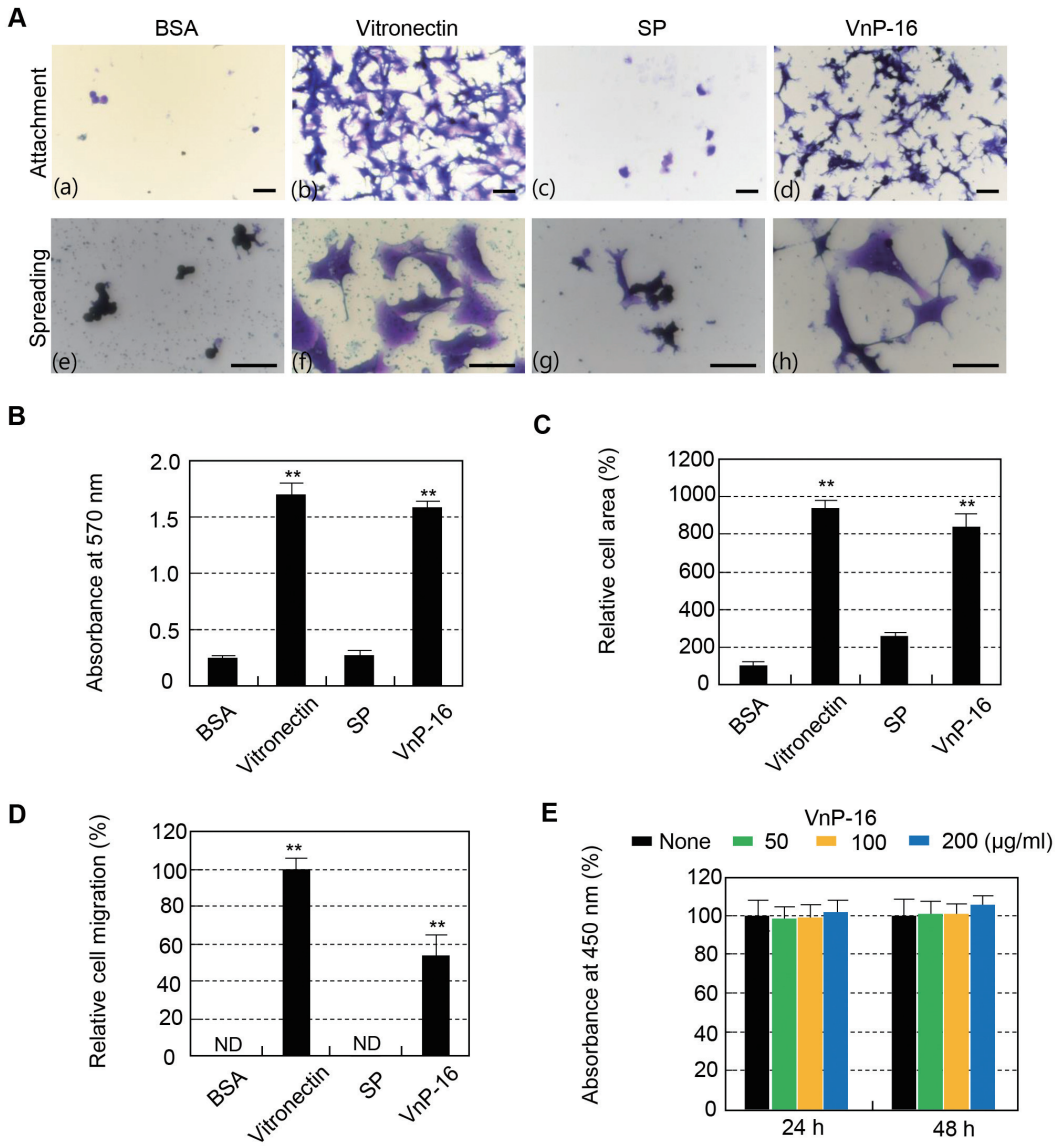

Figure 4. Cell attachment, spreading, and migration of human osteosarcoma (HOS) cells seeded on culture plates treated with vitronectin, scrambled peptide (SP) and VnP-16 peptide **(A)** Photographs of HOS cells adhering (a to d) and spreading (e to h) to culture plates treated with 1% bovine serum albumin (BSA), vitronectin (0.26 μg/cm^2), SP, and VnP-16 (10.5 μg/cm^2). Bar = 100 μm. **(B)** Cell attachment to immobilized vitronectin, SP and VnP-16. HOS cells were allowed to adhere to vitronectin-, peptide-treated plates for 1 h in serum-free medium. **(C)** Cell spreading to immobilized vitronectin, SP and VnP-16. HOS cells were allowed to adhere to vitronectin-, peptide-treated plates for 3 h in serum-free medium. **(D)** Migration of HOS cells induced by vitronectin, SP and VnP-16. HOS cells were seeded into the upper chambers of transwell filters coated with vitronectin (0.26 μg/cm^2), SP, or VnP-16 (10.5 μg/cm^2) and were incubated for 24 h. ND, not detected. **(E)** The viabilities of osteoblast-like HOS cells treated with VnP-16 for 24 or 48 h. No significant difference in absorbance according to VnP-16 concentration implied that VnP-16 was non-cytotoxic to the cells. $^{**}p < 0.01$ vs. the SP-treated control group. Data in **(B-E)** (n = 4) represent the mean + SD.

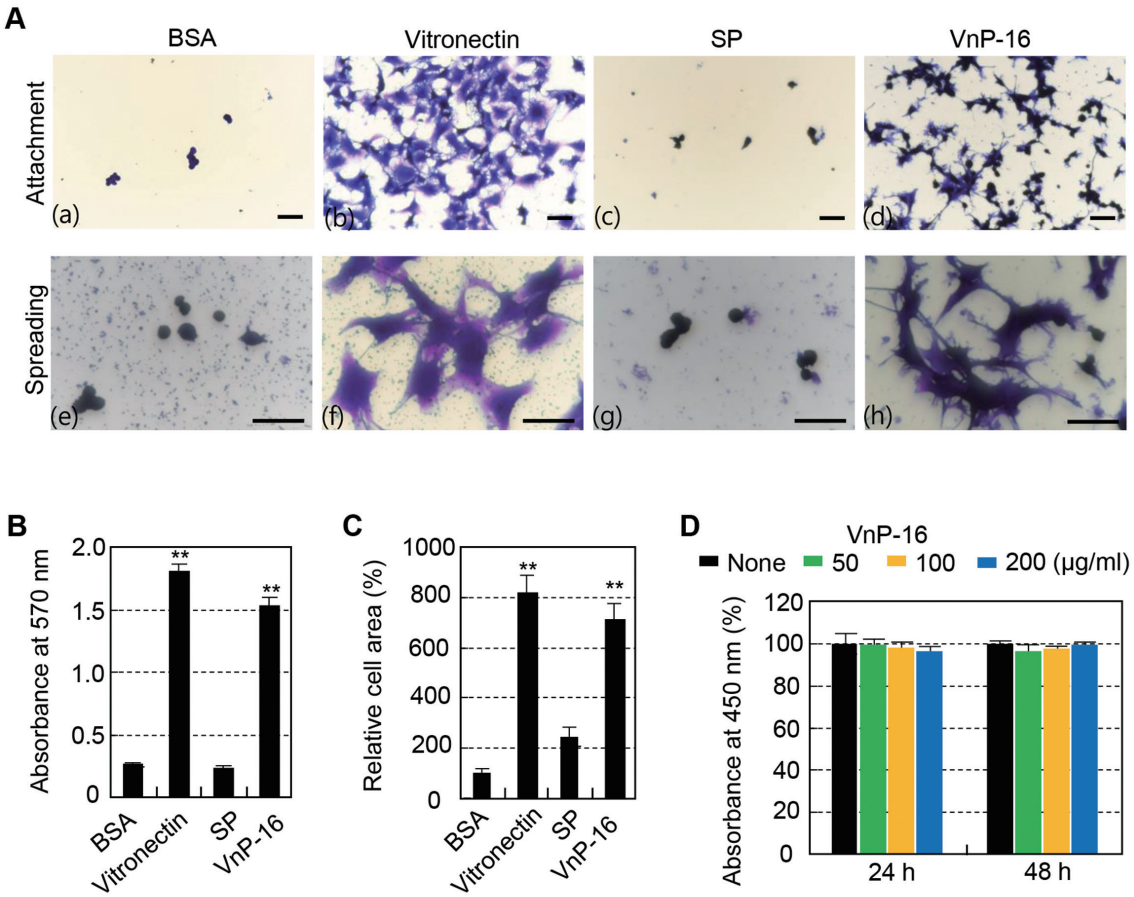

Figure 5. Cell attachment and spreading of osteoblast-like MG-63 cells seeded on culture plates treated with vitronectin, scrambled peptide (SP) and VnP-16 peptide. **(A)** Photographs of MG-63 cells adhering (a to d) and spreading (e to h) to culture plates treated with 1% bovine serum albumin (BSA), vitronectin (0.26 μg/cm^2), SP, and VnP-16 (10.5 μg/cm^2). Bar = 100 μm. **(B)** Cell attachment in response to immobilized vitronectin, SP and VnP-16. MG-63 cells were allowed to adhere to vitronectin-, peptide-treated plates for 1 h in serum-free medium. **(C)** Cell spreading in response to immobilized vitronectin, SP and VnP-16. MG-63 cells were allowed to adhere to vitronectin-, peptide-treated plates for 3 h in serum-free medium. **(D)** The viabilities of osteoblast-like MG-63 cells treated with VnP-16 for 24 or 48 h. No significant difference in absorbance according to VnP-16 concentration implied that VnP-16 was non-cytotoxic to the cells. $^{**}p < 0.01$ vs. the SP-treated control group. Data in **(B-D)** (n = 4) represent the mean + SD

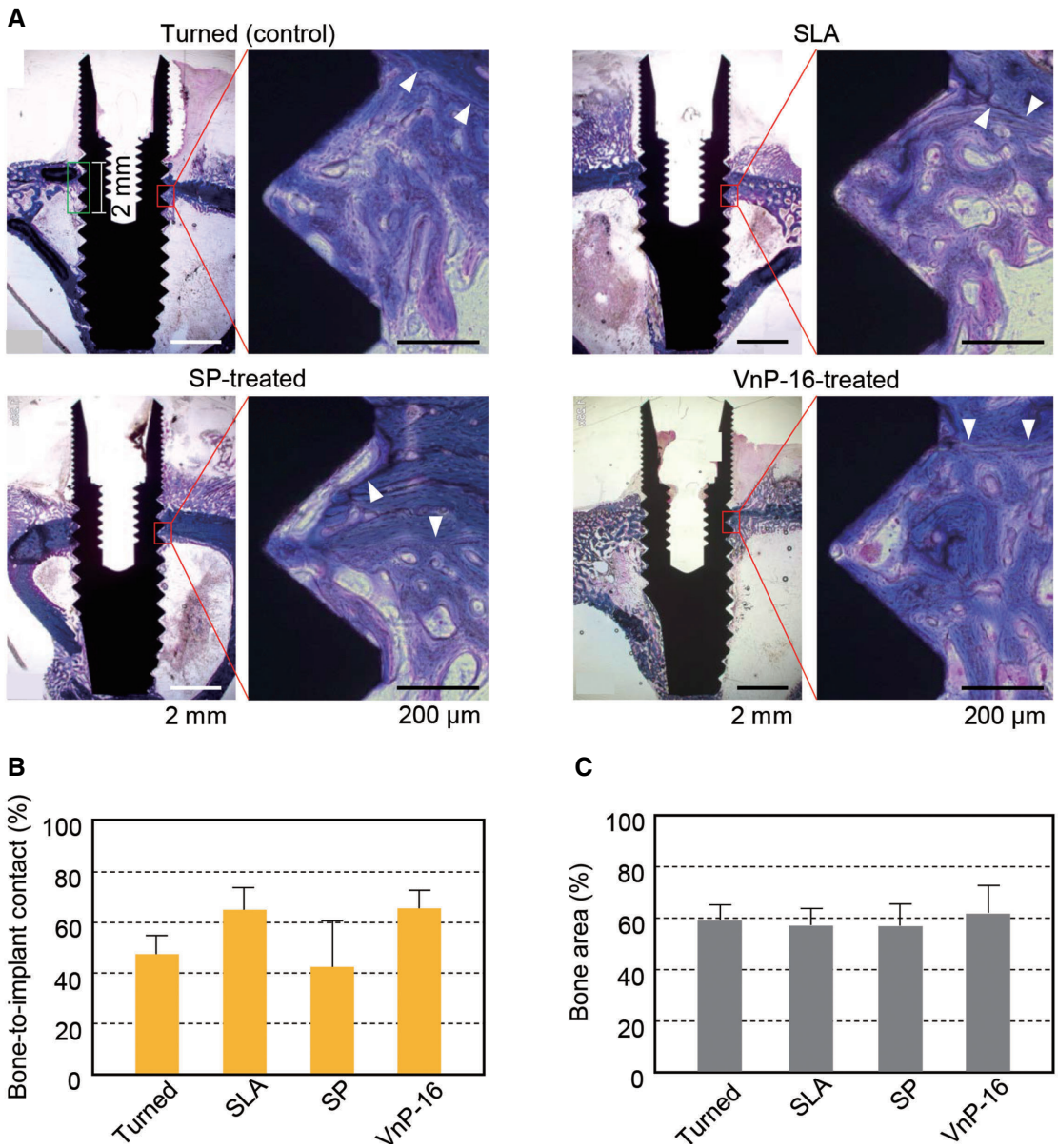

Figure 6. The histological views and histomorphometric data for bone responses to the turned, SLA, SP-treated SLA, and VnP-16-treated SLA titanium implant surfaces. **(A)** The demarcation lines (white arrowheads), difference in stained colors and maturity of the bone (cancellous or cortical), differentiate the new bone from the old bone. Here, the new bone is stained more reddish, whereas the old bone is stained more bluish. **(B)** The bone-to-implant contact ratios were measured, which are defined as the percentage of the implant surface in contact with bone to the total implant surface at the region of interest, which was the area ranging from the bone crest to 2 mm in depth in this study (green-edged rectangle in **(A)**, $p = 0.027$). **(C)** The ratio of the area filled with bone to the total area of the region of interest (bone area, or BA ratio) was also measured for each implant.

Table 5. The mean values ± standard deviation in histomorphometric data.

	Group			
	Turned	**SLA**	**SP**	**VnP-16**
BIC	47.0 ± 7.5	64.4* ± 8.6	42.1 ± 18.1	65.0* ± 7.2
BA	58.8 ± 6.0	56.8 ± 6.4	56.6 ± 8.4	61.5 ± 10.6

BIC : Bone-to-implant contact (%)
BA : Bone area (%)
* $p = 0.027$

4. Discussion

The results of this study demonstrated that the peptide VnP-16 induced initial cellular responses in human osteoblast-like cells, and the VnP-16-treated SLA titanium surface augmented the bone healing capacity in a dental implant in the early healing phase. The bioactive peptide VnP-16 is considered to promote early bone healing further when it is applied to the SLA titanium dental implant. VnP-16 is one of the candidate biomolecules that is clinically applicable for achieving stronger and faster osseointegration between the bone and titanium implant, together with some laminin-derived peptides.[12,15,20] As VnP-16 has the ability to both upregulate bone formation and downregulate bone resorption, unlike other peptides, the clinical availability of this material is expected to be high.[8]

Although extensive evidence indicates that the SLA titanium implant has long-term clinical performance with high survival rates (>95%),[25,26] this microroughened titanium surface has some weaknesses when installed to patients with a problem in bone metabolism such as osteoporosis.[27] VnP-16 can improve the bone healing response around the microroughened titanium implant without inducing immune responses, which has been demonstrated in the present study. The effect of VnP-16 on osseointegration of the SLA dental implant must be evaluated in normal and osteoporotic patients.

In this study, the physical adsorption method was used for the application of VnP-16 to culture plates and titanium surfaces. One of the primary advantages of this method is the simplicity, that is, it is a rapid and easy process to functionalize the titanium implant surface; however, this method has some drawbacks such as low effective peptide concentrations and denaturation of the three-dimensional structures of proteins or peptides.[19] The concentration of VnP-16 was determined from a dose-response curve through the cell attachment assay, as in a previous study (data not shown).[8] The lowest concentration, demonstrating the maximal effect on cell attachment, was used in this study, which solved the problem of the low effective peptide concentration. VnP-16, a sequence of only 12 amino acids, is interpreted to have no specific three-dimensional structure, which implies that it has low possibility of conformational change and the cellular responses induced by the small bioactive peptide are less affected by various cell types.[12,13] In addition, the other approaches to achieve peptide immobilization require

additional reaction time, caution, and costs.[19] Therefore, physical adsorption was the method of choice in this study despite several disadvantages. More effective methods are needed to be devised continuously.

In the analysis of surface chemistry in this study, the higher nitrogen contents observed on the peptide-treated surfaces imply that the peptide layers have been well-applied to the titanium implant surfaces. The most abundant element on the titanium surface was carbon in this study. This could be due to the biological aging of titanium surface under ambient conditions such as exposure to air.[28] However, the phenomenon of hydrocarbon contamination on the titanium surface had rarely affected the physical adsorption of the peptides used in this study.

Animal experiments were conducted on rabbits as described in a previous study.[20] It is known that rabbits are characterized by rapid growth and rapid bone turnover, which suggested the choice of a short experimental time to better focus on the effect of VnP-16 on the primary osteogenic activity. In the present study, the rabbits were adult and aged approximately 5-6 months, which would induce less growth-related response in the healing phase than that in immature rabbits.[29] Regarding bone remodeling aspects, an empirically derived, recommended duration of a remodeling cycle was approximately 6 weeks for rabbits, but 3-4 months for human beings, suggesting that a relative indicator, that is a factor of 3, is a good rule of thumb for extrapolating rabbit bone healing data to the clinical situation.[29] In this study, the rabbits were sacrificed at 2 weeks after implant insertion, which, for human beings, would be 6 weeks generally regarded as a standard of evaluating bone healing capacity in an early healing phase. Unfortunately, the BIC ratios in the present study revealed that there was no significant difference between the SLA- and VnP-16-treated implants, as other rabbit tibia model studies achieved no statistical significances at 10 days of sacrifice or longer.[3,20] Therefore, it is difficult to distinguish SLA-treated surface from the VnP-16-treated surface in an early healing phase between 2 weeks and a little earlier for rabbit experiments. Considering the rate of osseointegration in various models adopted (rabbit, dog, human), the fastest rate of osseointegration was observed in the rabbit model followed by the dog model. The slowest osseointegration rate was observed in humans.[30] More studies must be designed using larger mammals such as dogs to ensure that VnP-16 promotes bone formation in an early healing phase for more certainty.

Although the ANOVA test for BIC in this study showed a p value <0.05, the pairwise comparisons revealed no significant differences between the groups. Perhaps, the large SD, especially obtained from the measurements of the SP-treated implants, caused no significant differences in the pairwise comparisons. The high mean BIC ratios in the SLA- and VnP-16-treated groups and the low mean BIC in the turned and SP-treated groups could contribute to the significant difference in the ANOVA test in all the groups. The large SD of the data is due to the small sample size in this study. Another reason for the large SD might be the difficulty in displaying the entire three-dimensional bone-implant interface in light microscopic histology. The selection of one cross-sectional plane for light microscopy is arbitrary, and the data from the cross-section poorly correlated with the data measured on the entire three-dimensional image.[31] To obtain similar data between two- and three-dimensional images, at least three to four histological sections for each specimen are required, which are extremely difficult to prepare from an undecalcified specimen, including a tita-

nium implant.[32] Methodological advancements, such as three- dimensional imaging analysis by microcomputed tomography and grinding technique to prepare numerous histological sections from a small, hard specimen, are required to obtain more obvious in vivo results.

5. Conclusions

Within the limitations of this in vitro and in vivo study, the following conclusions can be drawn:

1. The in vitro results of this study indicate that VnP-16 accelerates the attachment and spreading of osteogenic cells, which may increase the bone healing capacity of SLA titanium surface without proliferating cell viability and cytotoxicity.
2. VnP-16 treatment resulted in remarkable histomorphometric osseointegration outcomes in the in vivo results without any foreign body reaction when applied to SLA titanium dental implant surface.

Based on the overall results of this study, a vitronectin-derived functional peptide, VnP-16, enhances the osteogenic potential of microroughened titanium dental implant surface.

6. Published paper related to this study

C.B. Cho, S.Y. Jung, C.Y. Park, H.K. Kang, I.L. Yeo, B.M. Min, A Vitronectin-Derived Bioactive Peptide Improves Bone Healing Capacity of SLA Titanium Surfaces. Materials 12(20) (2019) 3400. https://doi.org/10.3390/ma12203400

7. References

1. ROY, P., BERGER, S. & SCHMUKI, P. 2011. TiO_2 nanotubes: synthesis and applications. *Angew Chem Int Ed Engl*, 50, 2904-39.
2. THOMAS, K. A. & COOK, S. D. 1985. An evaluation of variables influencing implant fixation by direct bone apposition. *J Biomed Mater Res*, 19, 875-901.
3. CHOI, J. Y., KANG, S. H., KIM, H. Y. & YEO, I. L. 2018. Control variable implants improve interpretation of surface modification and implant design effects on early bone responses: An in vivo study. *Int J Oral Maxillofac Implants*, 33, 1033-1040.
4. WENNERBERG, A. & ALBREKTSSON, T. 2010. On implant surfaces: a review of current knowledge and opinions. *Int J Oral Maxillofac Implants*, 25, 63-74.
5. COCHRAN, D. L., BUSER, D., TEN BRUGGENKATE, C. M., WEINGART, D., TAYLOR, T. M., BERNARD, J. P., PETERS, F. & SIMPSON, J. P. 2002. The use of reduced healing times on ITI implants with a sandblasted and acid-etched (SLA) surface: early results from clinical trials on ITI SLA implants. *Clin Oral Implants Res*, 13, 144-53.
6. ROCCUZZO, M., BUNINO, M., PRIOGLIO, F. & BIANCHI, S. D. 2001. Early loading of sandblasted and acid-etched (SLA) implants: a prospective split-mouth comparative study. *Clin Oral Implants Res*, 12, 572-8.
7. Yeo, I.S. 2017. Surface modification of dental biomaterials for controlling bone response. *In Bone Response to Dental Implant Materials; Elsevier: Kidlington, Oxford, UK; pp.* 43-6.
8. MIN, S. K., KANG, H. K., JUNG, S. Y., JANG, D. H. & MIN, B. M. 2018. A vitronectin-derived peptide reverses ovariectomy-induced bone loss via regulation of osteoblast and osteoclast differentiation.

Cell Death Differ, 25, 268-281.

9. HOWLETT, C. R., EVANS, M. D., WALSH, W. R., JOHNSON, G. & STEELE, J. G. 1994. Mechanism of initial attachment of cells derived from human bone to commonly used prosthetic materials during cell culture. *Biomaterials*, 15, 213-22.
10. RIVERA-CHACON, D. M., ALVARADO-VELEZ, M., ACEVEDO-MORANTES, C. Y., SINGH, S. P., GULTEPE, E., NAGESHA, D., SRIDHAR, S. & RAMIREZ-VICK, J. E. 2013. Fibronectin and vitronectin promote human fetal osteoblast cell attachment and proliferation on nanoporous titanium surfaces. *J Biomed Nanotechnol*, 9, 1092-7.
11. SCOTCHFORD, C. A., BALL, M., WINKELMANN, M., VOROS, J., CSUCS, C., BRUNETTE, D. M., DANUSER, G. & TEXTOR, M. 2003. Chemically patterned, metal-oxide-based surfaces produced by photolithographic techniques for studying protein- and cell-interactions. II: Protein adsorption and early cell interactions. *Biomaterials*, 24, 1147-58.
12. YEO, I. S., MIN, S. K., KANG, H. K., KWON, T. K., JUNG, S. Y. & MIN, B. M. 2015. Identification of a bioactive core sequence from human laminin and its applicability to tissue engineering. *Biomaterials*, 73, 96-109.
13. CACCHIOLI, A., RAVANETTI, F., BAGNO, A., DETTIN, M. & GABBI, C. 2009. Human vitronectin-derived peptide covalently grafted onto titanium surface improves osteogenic activity: A pilot in vivo study on rabbits. *Tissue Eng Part A*, 15, 2917-26.
14. PETRIE, T. A., RAYNOR, J. E., DUMBAULD, D. W., LEE, T. T., JAGTAP, S., TEMPLEMAN, K. L., COLLARD, D. M. & GARCIA, A. J. 2010. Multivalent integrin-specific ligands enhance tissue healing and biomaterial integration. *Sci Transl Med*, 2, 45ra60.
15. KANG, H. K., KIM, O. B., MIN, S. K., JUNG, S. Y., JANG, D. H., KWON, T. K., MIN, B. M. & YEO, I. S. 2013. The effect of the DLTIDDSYWYRI motif of the human laminin alpha2 chain on implant osseointegration. *Biomaterials*, 34, 4027-4037.
16. REZANIA, A. & HEALY, K. E. 1999. Biomimetic peptide surfaces that regulate adhesion, spreading, cytoskeletal organization, and mineralization of the matrix deposited by osteoblast-like cells. *Biotechnol Prog*, 15, 19-32.
17. VUKICEVIC, S., LUYTEN, F. P., KLEINMAN, H. K. & REDDI, A. H. 1990. Differentiation of canalicular cell processes in bone cells by basement membrane matrix components: regulation by discrete domains of laminin. *Cell*, 63, 437-45.
18. MARTIN, L. J., AKHAVAN, B. & BILEK, M. M. M. 2018. Electric fields control the orientation of peptides irreversibly immobilized on radical-functionalized surfaces. *Nat Commun*, 9, 357.
19. Stewart, C., Akhavan, B., Wise, S.G., Bilek, M.M. 2019. A review of biomimetic surface functionalization for bone-integrating orthopedic implants: Mechanism, current approaches, and future directions. *Prog Mater Sci*, 106, 100588.
20. KIM, S., CHOI, J. Y., JUNG, S. Y., KANG, H. K., MIN, B. M. & YEO, I. L. 2019. A laminin-derived functional peptide, PPFEGCIWN, promotes bone formation on sandblasted, large-grit, acid-etched titanium implant surfaces. *Int J Oral Maxillofac Implants*, 34, 836-844.
21. KIM, J. M., MIN, S. K., KIM, H., KANG, H.

K., JUNG, S. Y., LEE, S. H., CHOI, Y., ROH, S., JEONG, D. & MIN, B. M. 2007. Vacuolar-type H+-ATPase-mediated acidosis promotes in vitro osteoclastogenesis via modulation of cell migration. *Int J Mol Med*, 19, 393-400.

22. KILKENNY, C., BROWNE, W. J., CUTHILL, I. C., EMERSON, M. & ALTMAN, D. G. 2010. Improving bioscience research reporting: the ARRIVE guidelines for reporting animal research. *PLoS Biol*, 8, e1000412.
23. DONATH, K. & BREUNER, G. 1982. A method for the study of undecalcified bones and teeth with attached soft tissues. The Sage-Schliff (sawing and grinding) technique. *J Oral Pathol*, 11, 318-26.
24. GRUBER, H. E. 1992. Adaptations of Goldner's Masson trichrome stain for the study of undecalcified plastic embedded bone. *Biotech Histochem*, 67, 30-4.
25. BUSER, D., JANNER, S. F., WITTNEBEN, J. G., BRAGGER, U., RAMSEIER, C. A. & SALVI, G. E. 2012. 10-year survival and success rates of 511 titanium implants with a sandblasted and acid-etched surface: a retrospective study in 303 partially edentulous patients. *Clin Implant Dent Relat Res*, 14, 839-51.
26. VAN VELZEN, F. J., OFEC, R., SCHULTEN, E. A. & TEN BRUGGENKATE, C. M. 2015. 10-year survival rate and the incidence of peri-implant disease of 374 titanium dental implants with a SLA surface: a prospective cohort study in 177 fully and partially edentulous patients. *Clin Oral Implants Res*, 26, 1121-8.
27. TSOLAKI, I. N., MADIANOS, P. N. & VROTSOS, J. A. 2009. Outcomes of dental implants in osteoporotic patients. A literature review. *J Prosthodont*, 18, 309-23.
28. CHOI, S. H., JEONG, W. S., CHA, J. Y., LEE, J. H., LEE, K. J., YU, H. S., CHOI, E. H., KIM, K. M. & HWANG, C. J. 2017. Overcoming the biological aging of titanium using a wet storage method after ultraviolet treatment. *Sci Rep*, 7, 3833.
29. ROBERTS, W. E., SMITH, R. K., ZILBERMAN, Y., MOZSARY, P. G. & SMITH, R. S. 1984. Osseous adaptation to continuous loading of rigid endosseous implants. *Am J Orthod*, 86, 95-111.
30. BOTTICELLI, D. & LANG, N. P. 2017. Dynamics of osseointegration in various human and animal models - a comparative analysis. *Clin Oral Implants Res*, 28, 742-748.
31. CHOI, J. Y., PARK, J. I., CHAE, J. S. & YEO, I. L. 2019. Comparison of micro-computed tomography and histomorphometry in the measurement of bone-implant contact ratios. *Oral Surg Oral Med Oral Pathol Oral Radiol*, 128, 87-95.
32. BERNHARDT, R., KUHLISCH, E., SCHULZ, M. C., ECKELT, U. & STADLINGER, B. 2012. Comparison of bone-implant contact and bone-implant volume between 2D-histological sections and 3D-SRmicroCT slices. *Eur Cell Mater*, 23, 237-47; discussion 247-8.

국문초록

인체유래 부착단백질 비트로넥틴에서 발굴한 기능성 펩타이드가 미세거칠기를 증가시킨 티타늄 임플란트 표면의 골형성능에 미치는 영향

지도교수 여 인 성

서울대학교 대학원
치의과학과 치과보철학 전공
조 창 빈

목적. 미세거칠기를 증가시킨 SLA 티타늄 임플란트는 치과 임상에서 우수한 골유착 결과를 보여주었으나 골다공증, 당뇨 같은 전신질환을 앓고 있는 환자들에 있어서도 우수한 골유착 결과를 얻기 위한 SLA 티타늄 임플란트 표면 개선이 여전히 필요하다. 이 연구에서는, 인체유래 부착단백질 비트로넥틴에서 발굴한 기능성 펩타이드 VnP-16이 SLA 티타늄 표면의 골형성능에 미치는 영향을 조사하였다.

방법. 생체외 실험에서는 다음의 네 가지 티타늄 디스크를 준비하여 surface topographgy 같은 물리적 특성과 surface chemistry 같은 화학적 특성을 비교하였다: 미세거칠기를 증가시키지 않은 무처리 티타늄 그룹, 미세거칠기만 증가시킨 티타늄 그룹, 미세거칠기를 증가시키고 무작위로 합성한 펩타이드로 표면처리한 티타늄 그룹, 미세거칠기를 증가시키고 VnP-16 표면처리한 티타늄 그룹. 또다른 생체외 실험에서는 마이크로플레이트에 무처리, 비트로넥틴, 무작위 합성 펩타이드, VnP-16 처리 후, 조골세포와 유사한 인간 골육종세포(human osteosarcoma cell, HOS cell)와 MG-63 cell의 세포 부착, 확장, 전이, 생존력 정도를 각각 비교하였다. 생체내 실험에서는 첫번째 생체외 실험과 같은 실험군, 대조군 임플란트를 토끼 경골에 식립한지 2주 후 비탈회 시편을 채취하여 광학현미경 사진과 조직계측학적 정량평가자료를 비교하였다.

결과. VnP-16 표면처리는 티타늄 디스크 표면의 물리적 특성을 변화시키지 않았다. 세포실험에서는 VnP-16 처리가 HOS cell과 MG-63 cell의 세포 부착, 확장 정도를 증가시켰으나, 세포독성이나 생존력 정도에는 영향을 미치지 않았다. 생체내 실험에서 VnP-16 표면처리한 SLA 임플란트는 골-임플란트 계면의 이물 반응이 없었고, 무작위 합성 펩타이드 표면처리한 임플란트에 비해 우수한 골-임플란트 접촉률을 보여주었다(p = 0.027).

결론. VnP-16은 미세거칠기를 증가시킨 SLA 티타늄 임플란트 표면의 골형성능을 증가시킨다.

주요어 : 비트로넥틴; 펩타이드; 세포부착; 티타늄; 골유착; 치과용 임플란트; 생체친화재료
학번 : 2014-30702

감사의 글

박사 과정을 마치고 이 논문을 완성하기까지 도움을 주신 교수님, 동료 및 선후배님들, 가족에게 진심으로 감사의 말씀을 전합니다.

의국세미나와 대학원 수업 때 세심한 조언과 격려, 지도해주신 치과보철학교실의 허성주 교수님, 한중석 교수님, 곽재영 교수님, 김성균 교수님, 임영준 교수님, 김명주 교수님, 권호범 교수님, 윤형인 교수님께 이 자리를 빌어 정말 감사드립니다.

바쁘신 와중에도 본 논문 심사를 위해서 열과 성을 다해주신 한중석 교수님, 윤형인 교수님과 치과생체재료과학교실의 안진수 교수님, 경희대학교 치과보철학교실의 배아란 교수님께도 다시 한번 감사드립니다.

곽재영 교수님, 학부생 때부터 지도 학생인 저를 아껴주시고 오며가며 항상 온화한 미소로 반겨주셔서 감사드립니다. 저희들이 부담 갖지 않도록 묵묵히 챙겨주시고 지켜봐 주신 덕분에 초심을 유지하고 박사 과정까지 무사히 끝마칠 수 있었습니다.

여인성 교수님, 스승님의 연구에 대한 열정과 연구를 대하는 태도에 존경을 표하며, 제자를 배려해 주시는 마음씨와 한결같으신 지도에 감사드립니다. 저도 후배님들에게 그러한 모습으로 기억될 수 있도록 더욱 정진하겠습니다. 작은 치과의원이지만 혼자서 챙겨야 할 일들이 많아 논문을 시작할 엄두를 못 내던 시절, 다시 한번 기회를 주시고 손수 이끌어 주셔서 여기까지 성장할 수 있었습니다. 박사 학위논문을 작업하면서 학업적인 연구에 대해 더 많이 배웠으며, 뿐만 아니라 임상을 대하는 태도 또한 더욱 진지해 진 것 같습니다. 미천한 능력이지만 뜻 깊은 곳에 쓰일 수 있도록 힘쓰겠습니다.

논문을 완성하기까지 모든 것을 혼자 힘으로만 해결할 수는 없었습니다. 도와주신 최정유 박사님, 치과보철학교실의 김웅규 선생님, 구강생화학교실의 정성윤 선생님께 깊은 감사를 드립니다.

박사과정 동안 늦은 밤과 주말에도 제가 드린 질문에 긴 시간 성심껏 답변을 주신 이재현 진료교수님과 김성진 박사님께도 감사의 말씀을 드립니다.

마지막으로 항상 저를 믿어주시고 많은 사랑과 정성으로 보살펴 주신 부모님과 가족들에게 감사드리며, 모든 분들의 가정에 평안과 행복이 깃들기를 희망합니다.

2020년 7월

조 창 빈